Functional neurogenesis in the adult hippocampus

Henriette van Praag*†, Alejandro F. Schinder*†‡, Brian R. Christie*†‡, Nicolas Toni*, Theo D. Palmer*‡ & Fred H. Gage*

** Laboratory of Genetics, The Salk Institute for Biological Studies, La Jolla, California 92037, USA*
† These authors contributed equally to this work

There is extensive evidence indicating that new neurons are generated in the dentate gyrus of the adult mammalian hippocampus, a region of the brain that is important for learning and memory[1–5]. However, it is not known whether these new neurons become functional, as the methods used to study adult neurogenesis are limited to fixed tissue. We use here a retroviral vector expressing green fluorescent protein that only labels dividing cells, and that can be visualized in live hippocampal slices. We report that newly generated cells in the adult mouse hippocampus have neuronal morphology and can display passive membrane properties, action potentials and functional synaptic inputs similar to those found in mature dentate granule cells. Our findings demonstrate that newly generated cells mature into functional neurons in the adult mammalian brain.

Hippocampal neurogenesis has been observed in adult animals from birds to humans[1–6]. The newly generated cells may have a function in cognition and brain repair. For example, manipulations that increase neurogenesis, such as an enriched environment[7] and exercise[8], are associated with improved memory function and enhanced synaptic plasticity[9]. In addition, new neurons are generated in the hippocampus after stroke[10] and seizures[11], and in the cortex after a selective lesion[12], suggesting that they may be involved in recovery from injury. Stress, on the other hand, has been related to decreased cell proliferation and memory impairment[13,14]. However, the conclusions from all of these studies are based on correlations. It is still unclear whether newly generated cells that express neuronal markers become functional neurons.

Embryonic hippocampal progenitors can develop neuronal electrophysiological properties and are able to form functional synapses in culture[15]. Furthermore, adult hippocampal progenitors display voltage-dependent currents *in vitro*[16,17]. It remains unknown whether newly generated cells become functional neurons *in vivo*, mainly owing to the methods currently available to study neurogenesis. Both tritiated thymidine[1,2,6] and 5-bromodeoxyuridine (BrdU)[3–5,7–9] are used to label dividing cells in the adult brain; however, both methods require processing of the tissue and only label the soma. To overcome these limitations, we used a retroviral vector expressing green fluorescent protein (GFP), which only labels dividing cells[18]. GFP fills the soma as well as the processes, making structural analysis possible. Moreover, GFP can be visualized under fluorescence microscopy, allowing functional characterization of newly generated cells in hippocampal slices. Using this methodology, we have identified one-month-old neurons with functional properties similar to those of mature dentate granule cells in the adult hippocampus. We also show that newly generated neurons are initially smaller and reach a more mature morphology after 4 months.

To label proliferating cells in the adult hippocampus, a highly concentrated retroviral stock (1.5 μl of 5×10^8 infectious units per ml) carrying the GFP transgene was injected into the dentate gyrus. One group of mice was housed with a running wheel[8] to enhance cell division before injection. Mice were killed after 48 h to assess cell phenotype shortly after proliferation, or after 4 weeks to determine cell fate. GFP-expressing (GFP^+) cells were found in the dentate gyrus after both 48 h and 4 weeks. GFP^+ cell counts revealed that, in contrast to BrdU, retroviral labelling is quite variable and, therefore, unsuitable for absolute quantitative comparisons between controls and experimental mice (hereafter referred to as runners) (see Methods). In spite of this caveat, a relatively high percentage of GFP^+cells expressed neuronal markers at 4 weeks in runners, making a detailed morphological and electrophysiological characterization of newly generated neurons possible (Table 1).

The phenotypes of the GFP^+cells were examined by immunofluorescent labelling for neuronal and glial markers. At 48 h after viral injection, GFP^+ cells were found to be immature neurons (Tuj1-β), neural precursors (NG2) or glia (GFAP), but not mature neurons (NeuN or calbindin; Fig. 1 and Table 1). About 50% of the GFP^+ cells remained unidentified. A portion of these cells may be associated with the vasculature[19]. Most GFP^+cells were located in the inner granule cell layers of the dentate gyrus, suggesting that the new cells arise from progenitors in the subgranular zone[3].

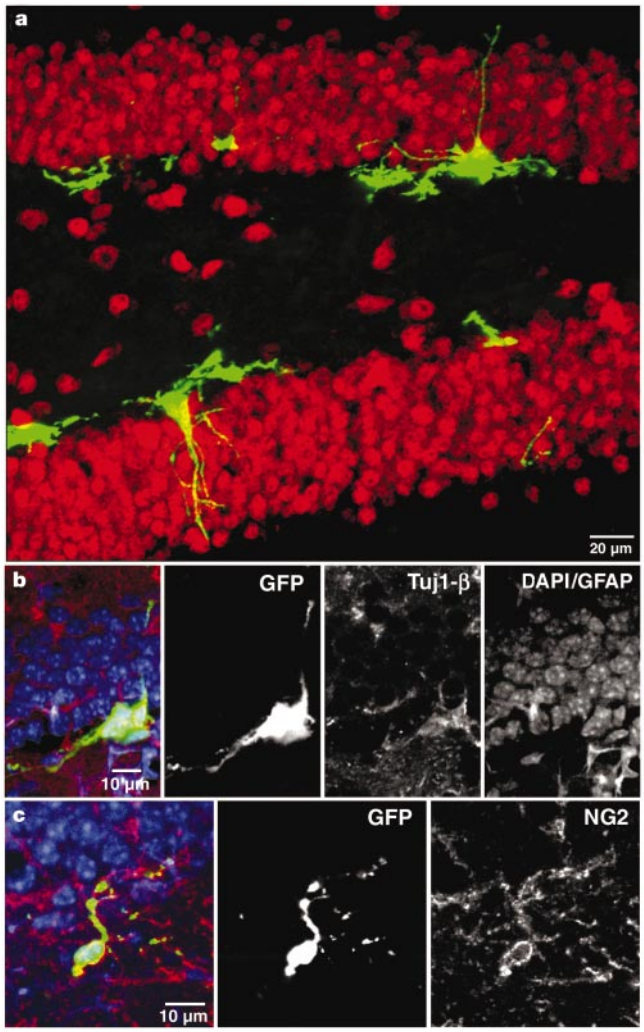

Figure 1 Dividing cells in the adult mouse dentate gyrus express early neural markers at 48 h after virus injection. **a**, Confocal micrograph (a merged image of 15 1-μm optical sections) of GFP expression in the dentate gyrus in a section that was labelled for the neuronal marker NeuN (red). No co-labelling of GFP^+ cells with NeuN was observed. **b**, Single confocal plane of a cluster of GFP^+ cells labelled with the early neuronal marker Tuj1-β (red). **c**, Single confocal plane of a GFP^+ cell with immunoreactivity for the progenitor marker NG2 (red). In **b** and **c**, nuclei (DAPI) and GFAP are blue.

‡ Present addresses: Instituto de Investigaciones Bioquímicas Fundación Campomar, Av. Patricias Argentinas 435, (1405) Buenos Aires, Argentina (A.F.S.); Department of Psychology and Neuroscience Program, University of British Columbia Vancouver, British Columbia, V6T 1Z4, Canada (B.R.C.); Department of Neurosurgery, Stanford University, California 94305, USA (T.D.P.).

Table 1 Number and phenotype of GFP$^+$ cells

Property of cells	Control 48 h ($n = 5$)	Running 48 h ($n = 5$)	Control 4 weeks ($n = 5$)	Running 4 weeks ($n = 8$)
GFP$^+$ cells	265 (66)	260 (45)	87 (22)	130 (38)
Spread (mm)	1.54 (0.16)	1.58 (0.16)	1.82 (0.28)	1.47 (0.21)
NeuN (%)	0	0	2.2 (1.3)	27.4 (9.3)**
Calbindin (%)	0	0	2.0 (1.2)	22.5 (9.3)**
Tuj1-β (%)	9.2 (1.1)	28.4 (8.3)*	15.6 (6.9)	31.7 (3.6)*
NG2 (%)	26.0 (12.2)	35.0 (2.3)*	7.7 (5.0)	13.7 (3.8)
GFAP (%)	4.1 (1.9)	4.6 (3.6)	10.3 (4.2)	8.6 (1.5)

The total number of GFP$^+$ cells from the dentate gyrus is shown at indicated time points after viral injection. At 48 h, runners had a greater percentage of GFP$^+$ cells labelled for Tuj1-β ($P < 0.04$) and NG2 ($P < 0.05$) than controls. At 4 weeks, the percentage of GFP$^+$ cells co-labelling with neuronal markers was significantly higher in runners than in controls (NeuN, $P < 0.01$; calbindin, $P < 0.01$; Tuj1-β, $P < 0.04$). All data are presented as means, with s.e.m. in parentheses. Asterisk, $P < 0.05$; double asterisk, $P < 0.01$.

Table 2 Morphological characteristics of GFP$^+$ newly generated granule cells

Morphological characteristic	Four-week-old neurons	Four-month-old neurons	Statistical significance (P)
Area of soma* (μm^2)	80.0 (5.6)	138 (14)	0.002
Total dendritic length (μm)	359 (45)	552 (49)	0.01
Number of branch points	4.1 (0.7)	6.8 (0.6)	0.01
Spine density† (μm^{-1})	0.77 (0.04)	1.19 (0.07)	0.0002

Data are presented as means, with s.e.m. in parentheses. The column on the right shows the statistical significance, calculated using a t-test. $n = 8$ for all characteristics, except spine density for 4-month-old neurons, where $n = 5$.
* Maximal cross-sectional area obtained from stereological measurements.
† Measured over a total dendritic length of 607 μm in newly generated cells at 4 weeks and 638 μm at 4 months after virus injection. The distances between the cell body and the beginning of the measured dendritic segments were similar for the 4-week-old (71 ± 9 μm) and 4-month-old (57 ± 5 μm) neurons ($P = 0.2$).

GFP$^+$cells expressing neuronal markers were found 4 weeks after injection (Table 1). Moreover, as GFP is expressed throughout the cytoplasm, dendritic processes extending towards and into the molecular layer and an axon projecting into the hilar area were observed (Fig. 2). Newly generated cells expressing neuronal markers were present throughout the granule cell layer (Figs 2a and 3a). The percentage of GFP$^+$cells that co-labelled with neuronal markers was significantly higher in runners (approximately 25%) than in controls (approximately 2%), supporting our previous observation that exercise enhances neurogenesis[8,9]. However, in both groups the percentages of GFP$^+$ neurons were lower than in the previous BrdU studies. This is probably due to differences in mechanisms of action between retrovirus and BrdU, or to transgene downregulation and/or shutdown of GFP expression. Downregulation may depend on the viral integration site into the genome of the host cell[20], and on the degree of differentiation of the cells. Indeed, GFP fluorescence was fainter in neuronal cells than in other cell types.

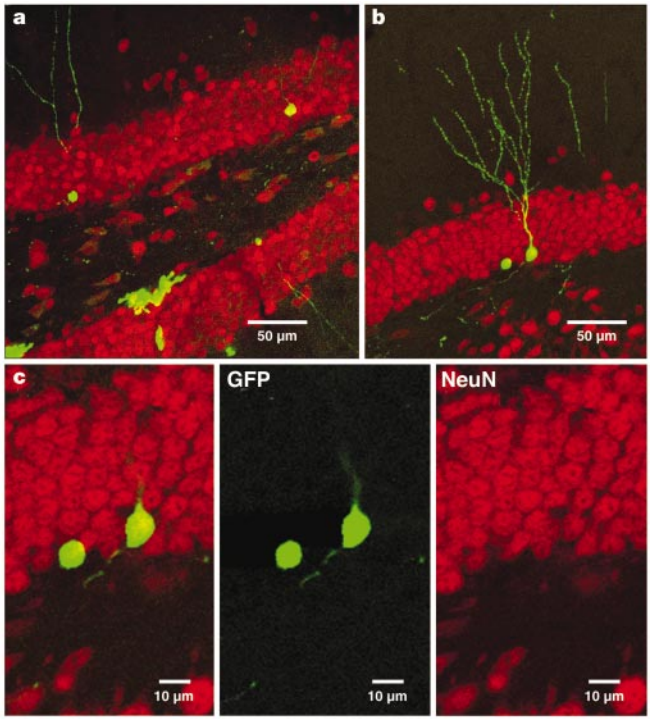

Figure 2 GFP$^+$ cells in the dentate gyrus 4 weeks after virus injection express mature neuronal markers. **a**, Overview of GFP expression in the dentate gyrus in a section (a merged image of 27 1-μm optical sections) that was labelled for the neuronal marker NeuN (red). **b**, GFP$^+$ cell (a merged image of 18 1-μm optical sections) immunoreactive for NeuN. **c**, Single confocal plane of the same cell, showing co-localization of GFP and NeuN.

To determine whether newborn neurons receive synaptic input, we carried out synaptophysin immunohistochemistry. Figure 3a shows a GFP$^+$, calbindin-positive cell with synaptophysin staining, consistent with previous studies[21]. Additional evidence for synaptic inputs is the presence of dendritic spines (Fig. 3b–e), suggesting that glutamate-containing terminals contact these dendrites[22]. Furthermore, ultrastructural analysis confirmed that newly generated granule cells do receive synaptic inputs[2]. The synapses of these newly generated granule cells express mature features such as a pool of presynaptic vesicles facing a postsynaptic density (Fig. 3f).

We have shown that newly generated cells can express mature neuronal markers and display the distinct morphology of a dentate granule neuron. To assess whether maturation continues, we compared the morphological characteristics of newly generated neurons at 4 weeks (Fig. 3d, e) and at 4 months (Fig. 3b, c) after retroviral injection. All measured parameters (size of soma, total dendritic length, dendritic branching and spine density) increased by about 60% over this period (Table 2). Thus, newly generated neurons in the adult grow and mature over several months. These findings are consistent with studies showing that spine density and dendritic complexity of dentate granule cells increase from birth well into adulthood[23]. Spine counts at 4 months were similar to those reported in the literature for mature neurons[24]. Thus, newborn neurons acquire the morphological dimensions of mature granule cells over several months. Of note, newly generated granule cells are functionally integrated into the circuitry by 4 weeks (see below).

To investigate whether newly generated neurons are functional, electrophysiological recordings of GFP$^+$ cells were made in acute hippocampal slices. Several GFP$^+$ cells showed neuronal properties (Table 3). In the example shown in Fig. 4, membrane potentials recorded in response to depolarizing current steps displayed

Table 3 Electrophysiological properties of newly generated and mature dentate granule cells

Electrophysiological property	Newly generated granule cells	n	Mature granule cells	n	Statistical significance (P)
Resting potential (mV)	–69.7 (1.7)	9	–74.8 (1.1)	27	0.06
Input resistance (MΩ)	350 (37)	11	388 (37)	25	0.62
Time constant (ms)	16.6 (4.0)	11	33.7 (3.7)	25	0.003
Membrane capacitance* (pF)	42.3 (10.2)	11	99.2 (12.7)	25	0.003
Spiking threshold (mV)	–45.8 (2.9)	13	–39.6 (1.5)	27	0.07
Firing rate† (Hz)	27.5 (2.6)	10	29.9 (4.8)	14	0.65
Spontaneous activity‡ (Hz)	1.6 (0.8)	6	0.80 (0.19)	9	0.33

Experiments on newly generated neurons (GFP$^+$) were carried out 4–8 weeks after viral injection. Data are presented as means, with s.e.m. in parentheses. The column on the right shows the statistical significance, calculated using a t-test.
* Calculated from the input resistance and the time constant, as $C_m = \tau_m/R_{in}$.
† Measured in response to a 100-pA depolarizing current step.
‡ Spontaneous postsynaptic responses measured in voltage or current clamp.

repetitive spiking with increasing frequency, reaching a plateau at about 140 Hz (Fig. 4b, d). Action potentials displayed a threshold (V_{th}) of −43 mV, conspicuous after hyperpolarization and frequency adaptation (Fig. 4b–d), similar to mature dentate granule cells under comparable recording conditions[25,26] (Fig. 5 and Table 3). To assess whether this cell had functional inputs, spontaneous postsynaptic currents were recorded (Fig. 4e). Currents displayed fast onset (less than 1 ms) and a slower exponential decay (greater than 5 ms), typical of postsynaptic responses to fast neurotransmitters, such as glutamate and γ-aminobutyric acid (GABA). Similar results were obtained in five additional experiments, where spontaneous postsynaptic responses were observed at a frequency of 0.4–5 Hz and with peak amplitudes ranging from 0.5 to 1 mV (under current clamp) and 10 to 20 pA (under voltage clamp; see Table 3). After fixation of the slice, co-labelling for GFP, Alexa Fluor 594 and NeuN showed that this cell had electrophysiological and morphological properties of a functional granule cell (Fig. 4f, g).

The main excitatory input to dentate granule cells is the perforant pathway. To assess whether newly generated neurons receive appropriate projections, postsynaptic currents were recorded in response to extracellular stimulation of the perforant path. Figure 5 depicts recordings from a GFP$^+$ cell and an adjacent mature granule cell with similar spiking properties. In both cells, excitatory postsynaptic currents were evoked in response to paired-pulse stimulation (Fig. 5c). Interestingly, although the same afferents were stimulated, the mature neuron displayed paired-pulse facilitation whereas the newly generated neuron showed depression, suggesting differences in presynaptic release properties. The observation that newly generated granule cells receive inputs from the perforant path ($n = 4$) strongly suggests that they are functionally integrated in the hippocampus.

A total of 13 GFP$^+$ cells with neuronal properties were characterized from 13 mice (Table 3). For comparison, recordings were carried out from 27 mature dentate granule cells obtained from 23 mice (Fig. 5 and Table 3). Most properties (resting potential (V_r), input resistance (R_{in}), threshold potential for spiking and firing rate) were found to be similar between the two groups. In addition, spontaneous postsynaptic responses (Fig. 4e and Table 3) displayed similar characteristics. Together with the observation that newly generated neurons receive inputs from the perforant path, these findings show a remarkable functional similarity between newly generated and mature granule cells.

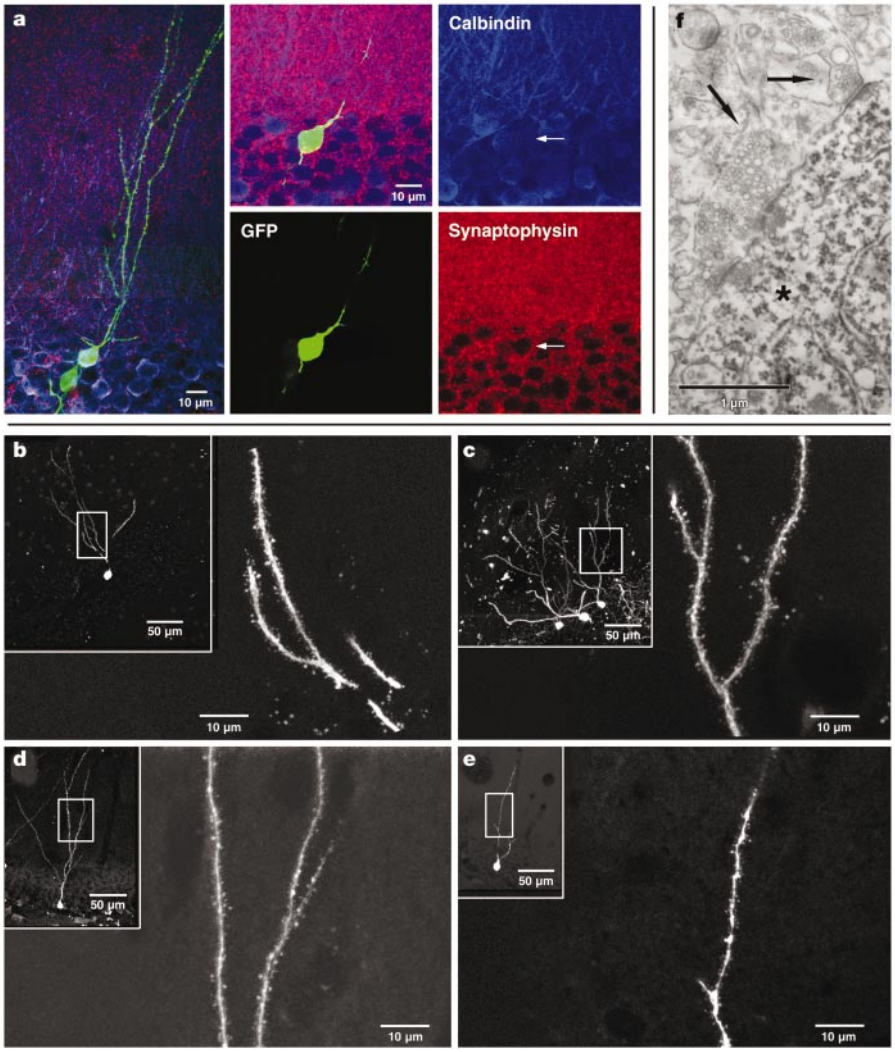

Figure 3 Newly generated neurons receive synaptic inputs. **a**, Confocal photomicrograph (a merged image of 10 0.5-μm optical sections) of a GFP$^+$ cell, immunolabelled for calbindin (blue) and synaptophysin (red). Adjacent panels (merged images of 4 0.5-μm optical sections) show co-localization with calbindin and synaptophysin. **b**–**e**, Visualization of spines in GFP$^+$ cells (merged images of 12–33 optical sections of 0.5 μm). The boxed areas in the insets correspond to the enlarged images of the dendrites. Cells were analysed 4 months (**b**, **c**) or 4 weeks (**d**, **e**) after virus injection. **f**, Electron micrograph of synaptic terminals (arrows) on the soma of a GFP$^+$ neuron (asterisk) in the granule cell layer.

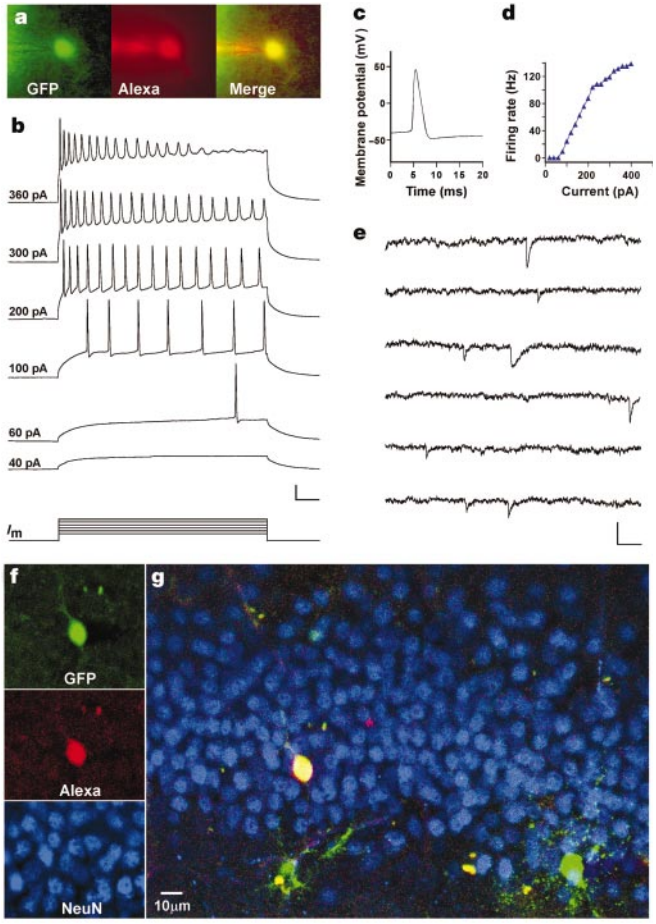

Figure 4 Newly generated cells display neuronal electrophysiological properties. **a**, Fluorescent micrographs of a GFP$^+$ cell filled with Alexa through a recording pipette. **b**, Membrane potential in response to depolarizing currents (I_m; 500 ms, 20–400 pA) recorded under current clamp at the resting potential (–73.5 mV). Numbers on the left indicate stimulus size. Scale: 25 mV, 50 ms. **c**, Action potential recorded at 80 pA. **d**, Firing rate versus current curve. **e**, Spontaneous postsynaptic currents recorded under voltage clamp (–80 mV). Scale: 20 pA, 100 ms. **f**, Confocal micrographs taken from a single plane (1 μm) after fixation of the slice. **g**, Overview of the dorsal blade of the granule cell layer (merged z-series of 23 planes).

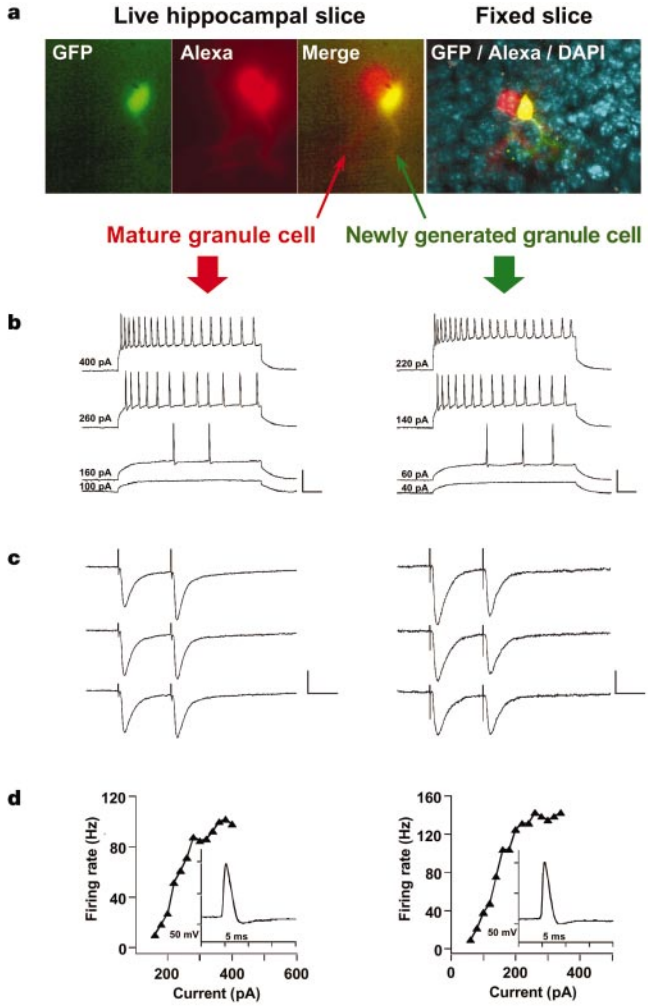

Figure 5 Newly generated neurons are functionally similar to mature dentate granule cells. Consecutive recordings of a GFP$^+$ neuron (right) and an adjacent granule cell (left) are shown. The GFP$^+$ neuron (C_m = 32 pF) was smaller and, therefore, younger than the unlabelled neuron (C_m = 60 pF). **a**, Fluorescence micrographs of both cells filled with Alexa (left panels). The right panel is a confocal micrograph taken after fixation, with GFP (green), Alexa (red) and DAPI (blue) visualized. **b**, Membrane potential in response to depolarizing current steps. Stimulus size is indicated on the left. Scale: 50 mV, 50 ms. **c**, Postsynaptic currents evoked by paired-pulse stimulation (100 μA, 0.2 ms, with a 50-ms interval) of the perforant path. The position of the stimulating electrode was identical for both neurons. Transients before the traces are stimulus artifacts. Scale: 100 pA, 25 ms (left); 40 pA, 25 ms (right). **d**, Spiking rate versus current curve. Insets show a single action potential.

The analysis of passive membrane properties (V_r, R_{in} and the time constant τ_m) revealed that newly generated neurons have a significantly faster τ_m compared with mature dentate granule cells (Table 3). The membrane capacitance (C_m), calculated as $C_m = \tau_m/R_{in}$, was found to be smaller in newly generated than in mature granule neurons, indicating that 4-week-old neurons are smaller than mature dentate granule cells[27] and confirming our own morphological observations (Fig. 5 and Table 2).

Recordings were performed from a total of 58 GFP$^+$ cells with different morphology and location in the dentate gyrus. All cells that displayed neuronal properties (n = 13) had a round soma located in the granule cell layer, dendrites extending towards the molecular layer, and, in general, low fluorescence intensity (Figs 4f and 5a). The additional 45 cells were non-excitable, had a markedly low R_{in} (209 ± 31 MΩ) and τ_m (9.8 ± 16 ms), and did not receive functional inputs. Typically, these cells had a large and irregular soma, multiple branches, and brighter fluorescence (data not shown). It is likely that these non-spiking cells represent a mixed population of neural precursors.

Our results demonstrate that the adult mammalian dentate gyrus gives rise to new functional neurons that are integrated into the hippocampal circuitry. It will be crucial to determine the functional significance of these newly generated cells in the adult brain. One possible hypothesis is that new neurons may be required to replace dying neurons[28]. Another possibility is that young neurons provide a greater degree of plasticity to the mature brain. This enhanced plasticity would become apparent from the integration of new functional units whose connectivity may be shaped by experience. □

Methods

Subjects and stereotaxic surgery

Female C57Bl/6 mice, 4–5 weeks old (Jackson Laboratories), were housed in standard conditions (n = 10) or with a running wheel (n = 80), four or five mice per cage. After one week, mice were anaesthetized (100 μg ketamine, 10 μg xylazine in 10 μl saline per gram) and virus (1.5 μl at 0.32 μl min^{-1}) was infused into the right dentate gyrus (anteroposterior = –2 mm from bregma; lateral = 1.5 mm; ventral = 2 mm). For electrophysiology (n = 53), another injection of virus (1.5 μl) was given in the same dentate gyrus (anteroposterior = –3 mm from bregma; lateral = 3 mm; ventral = 3 mm). Mice were killed 48 h,

4 weeks or 4 months after surgery for morphological experiments, and 4–8 weeks after injections for electrophysiology.

Immunocytochemistry

We carried out triple labelling on 40-μm free-floating coronal sections as described[3,19,21]. We applied antibodies in TBS with 3% donkey serum and 0.3% Triton X-100. Antibodies for NeuN (mouse monoclonal, 1:10), NG2 (rabbit polyclonal, Chemicon, 1:500) and GFAP (glialfibrillary acidic protein, guinea-pig polyclonal, Advanced Immunochemicals, 1:500) were combined. In additional series of sections, Tuj1-β (mouse monoclonal, BABCO, 1:500), calbindin (rabbit polyclonal, S Want, 1:500) and GFAP were pooled. Synaptophysin (mouse monoclonal, Boehringer-Mannheim, 1:50), calbindin and GFAP were also combined. Corresponding secondary antibodies (donkey anti-mouse Cy3, donkey anti-rabbit Cy5 and donkey anti-guinea-pig AMCA, 1:250) were used. We visualized nuclei with 4′-6-diaminodino-2-phenylindole (DAPI). For BrdU labelling, mouse anti-BrdU (Boehringer-Mannheim, 1:400) was used with biotinylated donkey anti-mouse (1:250) as a secondary antibody and diaminobenzadine as a chromagen (Vector Laboratories).

Cell quantification

Cells were counted using a confocal microscope (Bio-Rad) for GFP and a brightfield microscope (Leitz) for BrdU through a ×40 objective throughout the rostral–caudal extent of the granule cell layer in 1-in-6 series of 40-μm sections (240 μm apart). The total number of cells in the dentate gyrus was calculated on the basis of the multiple of the number of cells counted per hippocampus, and the sampling frequency.

Cell proliferation

To compare between effects of retrovirus and BrdU on cell proliferation, additional mice were used ($n = 5$ for runners, $n = 4$ for controls). After one week mice were given an intraperitoneal injection of BrdU (100 μg g^{-1}) and killed after 48 h. BrdU-positive cell number differed significantly between controls (964 ± 222) and runners (1,909 ± 306) ($P < 0.05$), suggesting that BrdU is preferable to retrovirus for cell quantification.

Spine density and soma measurements

Each GFP^+neuron that we used for spine counts was imaged at ×40 to obtain an overview. Dendrites were imaged through a ×100 objective with a digital zoom of 2. We merged z-series of 12–33 optical sections of 0.5 μm for the spine counts. Spines were defined by a visible neck and a spine head of at least 4 pixels. To quantify maximal cross-sectional somatic area, the total number of pixels was obtained using Adobe Photoshop. Measurements were carried out on merged z-series (12–18 1-μm optical sections) and then converted to μm^2.

Electron microscopy

GFP^+ cells in 100-μm sections were injected under a fluorescence microscope with 0.4% fluorescein-conjugated horseradish peroxidase (HRP, Sigma). Slices were processed for HRP[29], post-fixed in 1% osmium, and embedded in epoxy resin. Synapses were analysed on 35-nm thick serial sections on a jeol 100cxII electron microscope at 60 Kv, at a magnification of less than ×10,000.

Viral vector production

A retroviral vector based on the Moloney murine leukaemia virus expressing GFP was used. A stable NIT-GFP packaging cell line was generated as described previously[30]. Virus-containing supernatant was collected from clone 293gp/NIT-GFPc11 after transfection (Superfect, Qiagen) with pVSVG, and concentrated as described. Final virus titres were 5×10^8 neomycin-resistant (neo^r) colonies per ml of virus, as measured by G418-resistant colony formation on NIH 3T3 cells.

Electrophysiology

Four to eight weeks after surgery, runner mice were anaesthetized and decapitated. Brains were removed into a chilled solution containing (in mM): 110 choline Cl^-, 2.5 KCl, 1.3 NaH_2PO_4, 25.0 $NaHCO_3$, 0.5 $CaCl_2$, 7 $MgCl_2$, 20 dextrose, 1.3 Na^+ ascorbate, 0.6 Na^+ pyruvate, 5.5 kynurenic acid. Slices (200–400 μm thick) were cut as described previously[9], transferred to a chamber containing artificial cerebrospinal fluid (in mM: 125.0 NaCl, 2.5 KCl, 1.3 NaH_2PO_4, 25.0 $NaHCO_3$, 2 $CaCl_2$, 1.3 $MgCl_2$, 1.3 Na^+ ascorbate, 0.6 Na^+ pyruvate, 10 dextrose), bubbled with 95% O_2/5% CO_2 (pH 7.4, 320 mOsm), and stored at 30 °C. Using fluorescein optics (Leica DMLFS), slices were scanned for GFP^+ cells in the dentate gyrus. Microelectrodes (6–8 MΩ) were pulled from borosilicate glass (KG-33, Garner Glass) and filled with (in mM): 120.0 potassium gluconate, 20 KCl, 5 NaCl, 4 $MgCl_2$, 0.1 EGTA, 10.0 HEPES, 4.0 Tris-ATP, 0.3 Tris-GTP, 10 phosphocreatine (pH 7.4, 295 mOsm).

Whole-cell recordings (Axopatch 200B, Axon Instruments) were filtered at 2 kHz, digitized and acquired onto a PC using Labview-based acquisition and analysis software (L. Campbell, Salk Institute). Series resistance was typically 10–30 MΩ. We delivered stimuli at 5-s intervals. Criteria to include cells in the analysis were: (1) co-labelling with Alexa Fluor 594 (10 μg ml^{-1}, Molecular Probes) or visual confirmation of GFP in the pipette tip; (2) resting potential less than −50 mV; and (3) leak current less than 300 pA. Firing rate was calculated as the inverse of the inter-spike interval between the first 2 spikes of the train. We calculated τ_m by fitting a single exponential function to the membrane potential traces. Extracellular stimulation was done using a concentric bipolar electrode (50-μm diameter; FHC) and a stimulus isolation amplifier (Getting Instruments). After recording, slices were stored in 4% paraformaldehyde for over 24 h and processed for NeuN, followed by confocal analysis. We used GFP-negative dentate granule cells of slices from mice injected with virus as controls.

Received 6 November 2001; accepted 2 January 2002.

1. Altman, J. & Das, G. D. Autoradiographic and histological evidence of postnatal neurogenesis in rats. *J. Comp. Neurol.* **124,** 319–335 (1965).
2. Kaplan, M. S. & Hinds, J. W. Neurogenesis in the adult rat: electron microscopic analysis of light radioautographs. *Science* **197,** 1092–1094 (1977).
3. Kuhn, H. G., Dickinson-Anson, H. & Gage, F. H. Neurogenesis in the dentate gyrus of the adult rat: age-related decrease of neuronal progenitor proliferation. *J. Neurosci.* **16,** 2027–2033 (1996).
4. Kornack, D. R. & Rakic, P. Continuation of neurogenesis in the hippocampus of the adult macaque monkey. *Proc. Natl Acad. Sci. USA* **96,** 5768–5773 (1999).
5. Eriksson, P. S. *et al.* Neurogenesis in the adult human hippocampus. *Nature Med.* **4,** 1313–1317 (1998).
6. Barnea, A. & Nottebohm, F. Seasonal recruitment of hippocampal neurons in adult free-ranging black-capped chickadees. *Proc. Natl Acad. Sci. USA* **91,** 11217–11221 (1994).
7. Kempermann, G., Kuhn, H. G. & Gage, F. H. More hippocampal neurons in adult mice living in an enriched environment. *Nature* **386,** 493–495 (1997).
8. van Praag, H., Kempermann, G. & Gage, F. H. Running increases cell proliferation and neurogenesis in the adult mouse dentate gyrus. *Nature Neurosci.* **2,** 266–270 (1999).
9. van Praag, H., Christie, B. R., Sejnowski, T. J. & Gage, F. H. Running enhances neurogenesis, learning and long-term potentiation in mice. *Proc. Natl Acad. Sci. USA* **96,** 13427–13431 (1999).
10. Liu, J., Solway, K., Messing, R. O. & Sharp, F. R. Increased neurogenesis in the dentate gyrus after transient global ischemia in gerbils. *J. Neurosci.* **18,** 7768–7778 (1998).
11. Parent, J. M. *et al.* Dentate granule neurogenesis is increased by seizures and contributes to aberrant network reorganization in the adult hippocampus. *J. Neurosci.* **17,** 3727–3738 (1997).
12. Magavi, S. S., Leavitt, B. R. & Macklis, J. D. Induction of neurogenesis in the neocortex of adult mice. *Nature* **405,** 951–955 (2000).
13. Gould, E., Cameron, H. A., Daniels, D. C., Wooley, C. S. & McEwen, B. S. Adrenal hormones suppress cell division in the adult rat dentate gyrus. *J. Neurosci* **12,** 3642–3650 (1992).
14. Lemaire, V., Koehl, M., Le Moal, M. & Abrous, D. N. Prenatal stress produces learning deficits associated with an inhibition of neurogenesis in the hippocampus. *Proc. Natl Acad. Sci. USA* **97,** 11032–11037 (2000).
15. Vicario-Abejon, C., Collin, C., Tsoulfas, P. & McKay, R. D. Hippocampal stem cells differentiate into excitatory and inhibitory neurons. *Eur. J. Neurosci.* **12,** 677–688 (2000).
16. Sah, D. W., Ray, J. & Gage, F. H. Regulation of voltage- and ligand-gated currents in rat hippocampal progenitor cells *in vitro*. *J. Neurobiol.* **32,** 95–110 (1997).
17. Roy, N. S. *et al. In vitro* neurogenesis by progenitor cells isolated from the adult hippocampus. *Nature Med.* **6,** 271–277 (2000).
18. Lewis, P. F. & Emerman, M. Passage through mitosis is required for oncoretroviruses but not for the human immunodeficiency virus. *J. Virol.* **68,** 510–516 (1994).
19. Palmer, T. D., Willhoite, A. R. & Gage, F. H. Vascular niche for adult hippocampal neurogenesis. *J. Comp. Neurol.* **425,** 479–494 (2000).
20. Xu, L., Yee, J. K., Wolff, J. A. & Friedmann, T. Factors affecting long-term stability of Moloney murine leukemia virus-based vectors. *Virology* **171,** 331–341 (1989).
21. Markakis, E. A. & Gage, F. H. Adult-generated neurons in the dentate gyrus send axonal projections to field CA3 and are surrounded by synaptic vesicles. *J. Comp. Neurol.* **406,** 449–460 (1999).
22. Edwards, F. A. Anatomy and electrophysiology of fast central synapses lead to a structural model for long-term potentiation. *Physiol. Rev.* **75,** 759–787 (1995).
23. Crain, B., Cotman, C., Taylor, D. & Lynch, G. A quantitative electron microscopic study of synaptogenesis in the dentate gyrus of the rat. *Brain Res.* **63,** 195–204 (1973).
24. Suzuki, F., Makiura, Y., Guilhem, D., Sorensen, J. C. & Onteniente, B. Correlated axonal sprouting and dendritic spine formation during kainate-induced neuronal morphogenesis in the dentate gyrus of adult mice. *Exp. Neurol.* **145,** 203–213 (1997).
25. Staley, K. J., Otis, T. S. & Mody, I. Membrane properties of dentate gyrus granule cells: comparison of sharp microelectrode and whole-cell recordings. *J. Neurophysiol.* **67,** 1346–1358 (1992).
26. Lübke, J., Frotscher, M. & Spruston, N. Specialized electrophysiological properties of anatomically identified neurons in the hilar region of the rat fascia dentate. *J. Neurophysiol.* **79,** 1518–1534 (1998).
27. Coleman, P. A. & Miller, R. F. Measurement of passive membrane parameters with whole-cell recording from neurons in the intact amphibian retina. *J. Neurophysiol.* **61,** 218–230 (1989).
28. Biebl, M., Cooper, C. M., Winkler, J. & Kuhn, H. G. Analysis of neurogenesis and programmed cell death reveals a self-renewing capacity in the adult rat brain. *Neurosci. Lett.* **291,** 17–20 (2000).
29. Coleman, L. A. & Friedlander, M. J. Intracellular injections of permanent tracers in the fixed slice: a comparison of HRP and biocytin. *J. Neurosci. Methods* **44,** 167–177 (1992).
30. Palmer, T. D., Markakis, E. A., Willhoite, A. R., Safar, F. & Gage, F. H. Fibroblast growth factor-2 activates a latent neurogenic progam in neural stem cells from diverse regions of the adult CNS. *J. Neurosci.* **19,** 8487–8497 (1999).

Acknowledgements

We are grateful for the assistance of L. R. Kitabayashi and J. Simon in preparing the figures. We thank E. Bushong for assistance with electron microscopy, and N. Manison and R. Summers for help with confocal imaging. We also thank D. Cuizon, S. Forbes, M. Matthews, B. Miller and L. Moore for technical help, and M. L. Gage and K. Ganguly for comments on the manuscript. N.T. is supported by the Swiss Research Foundation. This work was supported by grants from the National Institutes of Health, Christopher Reeve Paralysis Foundation, and The Lookout Fund.

Competing interests statement

The authors declare that they have no competing financial interests.

Correspondence should be addressed to H.v.P.
(e-mail: vanpraag@salk.edu).